An experimental study of turbulence generation and decay in Taylor-Couette system due to an abrupt stoppage

Harminder Singh, A Prigent, Innocent Mutabazi

An experimental study of turbulence generation and decay in Taylor-Couette system due to an abrupt stoppage

Harminder Singh, A Prigent, & Mutabazi

An experimental study of turbulence generation and decay in Taylor-Couette system due to an abrupt stoppage

H. Singh[1], A. Prigent[1] & I. Mutabazi[1]

Laboratoire des Ondes et Milieux Complex (LOMC) CNRS UMR 6294, Université Le Havre, 75 Rue Bellot, Le Havre 76600, France
harminder.singh@univ-lehavre.fr

Résumé. Cette étude présente une approche novatrice de la génération et de la décroissance de la turbulence dans l'écoulement de Taylor-Couette, l'écoulement entre deux cylindres coaxiaux en rotation. A partir d'un écoulement initialement laminaire, les cylindres sont soumis à un arrêt brutal qui génère l'apparition de turbulence transitoire. Deux approches expérimentales complémentaires, les visualisations et les mesures de vitesse par stéréo-PIV, ont été utilisées pour mieux comprendre le phénomène présenté pour plusieurs vitesses initiales de rotation correspondant toujours à un écoulement laminaire. Trois configurations différentes peuvent être distinguées : rotation du cylindre extérieur seulement, co-rotation et contra-rotation. Lorsque seul le cylindre extérieur est en rotation, le seuil d'apparition de la turbulence correspond à un nombre de Reynolds extérieur initial $Re_o = 606$. En co- ou contra- rotation, ce seuil diminue jusqu'à une valeur minimale de $Re_o = 433$. Dans tous les cas, le retour à l'écoulement laminaire est plus lent qu'en stoppant le système à partir d'un écoulement turbulent. Contrairement à l'étude de Verschoof *et al.* [12], une décroissance auto-similaire de la turbulence n'a pas été observée.

Abstract. This study presents an innovative approach towards the generation and decay of turbulence in the Taylor-Couette system. The cylinders were brought to an abrupt stoppage that generated turbulence in the system, which was initially in the laminar flow region. Two complementary experimental approaches, namely visualizations and stereo-PIV measurements, were used to better understand the presented phenomenon for three different configurations at multiple rotation rates but always starting in the laminar flow region : only external cylinder, co-rotation and counter-rotation. For only external cylinder rotation, the lowest threshold limit of outer Reynolds number to was found to be $\Re_o$=606, which could be lowered with co- or counter-rotation to a minimal value of $\Re_o$=433. Nevertheless, the return to the laminar state is much slower in comparison to an abrupt stoppage from a turbulent state. In contrast to the study of Verschoof *et al.* [12], self-similar decay of turbulence was not observed.

1 Introduction

The interest in decay of turbulence in the scientific community was initiated by Taylor [1] by presenting his theory of decay of turbulence in a Windstream. It formed the base for the theoretical studies of homogeneous isotropic turbulence by Karman and Howarth [2], Kolmogorov [3] and Batchelor and Townsend [4],[5]. In the early nineties, George [6] presented a general theory for the decay of turbulence which coincided with the earlier theories presented by Karman and Howarth, Kolmogorov and Batchelor and Townsend when the respective assumptions were taken into consideration. George [6] demonstrated that the kinetic energy, which decays as a power law w.r.t. time, and the Taylor microscale, which increases as a square root of time, should be used as the scaling parameters to represent all scales of motion. George [6] strongly suggested the importance of initial conditions in determining the decay rate constant which they didn't find to be universal apart from the infinite Reynolds number limit.

However, turbulence in itself represents chaos and is therefore, generally, neither homogenous nor isotropic. Therefore, in recent years, some research has been conducted towards the wall-bounded turbulence decay to observe this chaotic behavior either numerically [7], [8] [9], [10] or experimentally [11],[12]. All of these studies have been conducted in different types of geometries : Pipe flow [11], two plates [7], 2D structures [8], T-mixer [10], and Taylor-Couette (TC) system [12], [9]. Each geometrical system has their own advantages, but the TC system, in which flow is contained between two concentric cylinders,

presents itself as the ideal system because it is a confined and closed system with nonhomogeneous and anisotropic turbulence [13]. The biggest advantage of the TC system over the pipe flow is its modest size which makes it more practical to study decay in a wall-bounded environment both experimentally and numerically.

Verschoof *et al.* (2016) [12] studied experimentally using PIV and LDA the decay in turbulence by stopping the inner cylinder, while outer cylinder was at rest, and allowing the turbulence to decay from the ultimate turbulent regime at Reynolds number of 106. However, they faced a practical problem of stopping the cylinder instantaneously which took 12s to reach a complete stop and during this time they didn't not measure the decay. Consequently, the group provided a follow-up numerical study [9] in which the inner cylinder was brought to a halt abruptly. As described by Batchelor and Townsend [4],[5], they [9] also observed three distinctly different stages of decay : initial, intermediate and final, but with different characteristics apart from the final decay stage which remains purely viscous.

In this manuscript, a slightly different phenomenon is presented. Instead of starting from the a turbulent flow and studying its decay, we started from a laminar flow. The rotation of the cylinders was fixed in order to obtain a laminar flow and after five minutes the cylinders were stopped instantaneously. Generation of turbulence was observed shortly after the stoppage which decayed afterwards due to absence of any further driving force given to the system. As a result, this experimental work differs significantly from the experimental work of Verschoof *et al.* [12] according to the following points : 1) flow was in laminar state before the instantaneous stoppage in comparison to turbulent state ; 2) Either outer or both cylinders in counter- or co- rotation were stopped instantaneously in comparison to only inner cylinder being stopped gradually ; 3) Cylinder were stopped instantaneously in comparison to gradual stoppage ; and 4) both the turbulence generation and decay are studied in comparison to just turbulence decay. This turbulence generation and decay is studied experimentally using two complementary approaches : visualizations with Kalliroscope and stereo-PIV measurements to capture all the three velocity components.

2 Methodology

The TC system consists of two cylinders with inner and outer radii of r_i=0.04 m and r_o=0.05 m, respectively, with a radius ratio, η=r_i/r_o, of 0.8 and gap width, d=$r_i - r_o$, of 0.01 m. The maximum height of the working fluid, L, is 0.45 m with aspect ratio Γ=L/b=45. Degasified water was used as the working fluid at a constant temperature of 20 °C maintained at both the inner and outer cylinder walls using water circulation. The inner cylinder (IC) is made of aluminum having black anodized wall to avoid reflection when working with laser. The outer cylinder is made of Plexiglas to provide optical access over the entire gap width axially. An optical access is also available from the top-plate to capture the $r - \theta$ plane for 2D-PIV measurements. The system also contains a bottom ring, attached to the outer cylinder with at a distance of 0.5 mm from the inner cylinder, and a top plate to reduce Ekman pumping. Three different set-ups were used at different rotational velocities : only outer cylinder rotating, co-rotation and counter-rotation. In each case, the flow conditions were laminar before stopping the cylinders abruptly.

In order to visualize flow structures, the water was initially degasified to get rid of bubbles and then mixed with 1 % Kalliroscope ST-1000. A r-z plane was illuminated with a class 4 Dantec Dyanmics Ray Power 2000 continuous laser with a maximum output of 4 W at 532 nm wavelength. This r-z plane was captured with a M series speed-sense CMOS camera of 4MP resolution and 800 fps speed using an objective of 105 mm. The Dantec Dynamics studio version 6.0 was used to capture and export the images which were then treated with Matlab R2018a software to obtain the presented results. A maximum of 2000 to 10000 single frame images were captured depending upon the acquisition frequency of 50 and 200 Hz (at higher Reynolds number), respectively.

The Stereo-PIV measurements were also done in the r-z plane through the transparent outer cylinder using two M series speed-sense CMOS camera of 4MP resolution and 800 fps speed using an objective of 105 mm. The cameras were synchronized with a Nd :YAG medium Class 4 Dantec Dynamics Litron laser LPY 50-200 having maximum output of 200 mJ, wavelength of 1064 nm, and a maximum frequency of acquisition of 200 Hz. However, in order to capture at least 35 seconds of the process, 50 Hz and 100 Hz (at higher Reynolds numbers) frequency of acquisitions were used to capture around 2500 and 3800

double image pairs, respectively. The fluid was seeded with fluorescent Rhodamine particles of average size between 5-20 μm. The calibration of both cameras was done with the pinhole method of the image modeling fit methodology using a special mire manufactured by the Dantec dynamics for stereo-PIV measurements for this specific TC system. The captured images were analyzed initially with the Dantec Dynamics studio version 6.0 to compute the vector fields using the adaptive PIV method having the maximum interrogation area size of 64×64 grid, minimum interrogation area size of 8×8 grid and grid step size of 4×4. Afterwards, the calibrations of both cameras were selected along with the vector fields of both cameras to create the stereo-PIV vector fields which were imported as *.txt files and treated with Matlab R2018a software to present the results.

3 Results & Discussion

First of all, some results of the visualization study with Kalliroscope are presented as space time diagrams at different starting inner and outer Reynolds numbers in Fig. 1. In Fig. 1a the evolution of generation of turbulence can be seen when inner cylinder was kept at a constant value of zero with increase in the outer Reynolds number ; on the other hand, in Fig. 1b the outer cylinder rotation is kept at a constant value either in co-current or counter-current while the inner Reynolds number is changed. The minimum $Re_o = \omega_o d/\nu$ at which turbulence generation and decay was observed is 606 without co- or counter-rotation. With the addition of co- or counter- rotation, the minimum Re_o at which turbulence generation and decay could be observed was found to be 433.

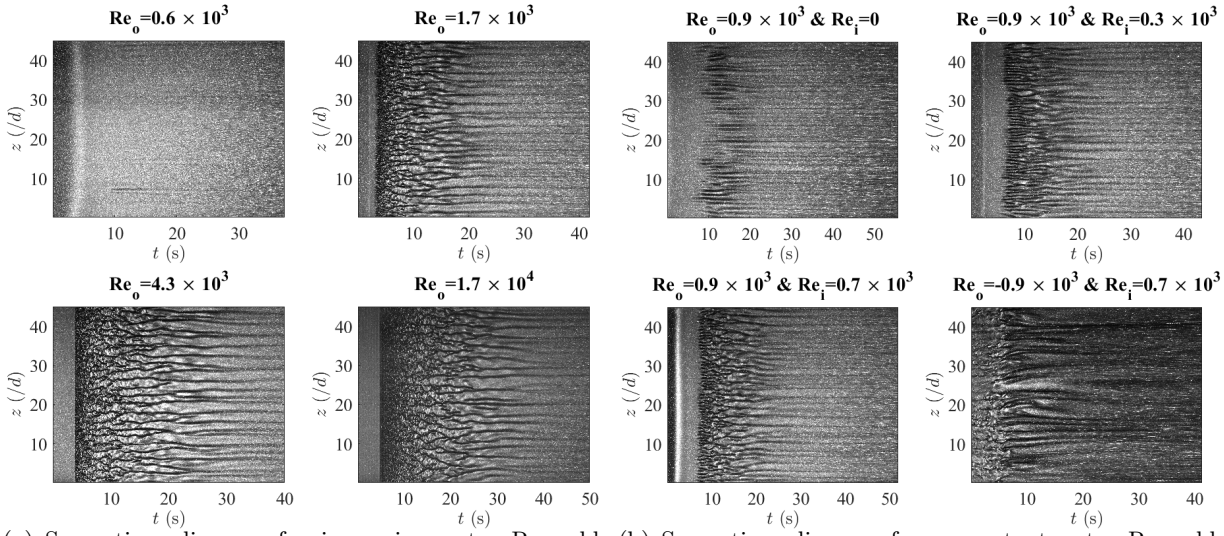

(a) Space-time diagram for increasing outer Reynolds number at zero inner reynolds number

(b) Space-time diagram for a constant outer Reynolds number and varying inner reynolds number

Figure 1. Space time diagrams at different inner and outer Reynolds number

It can be seen that at higher Re_o, the point of stoppage generates turbulence instantly throughout the axial length. Turbulence zone and consequently the decay time increases gradually with each increase in the Reynolds number. It was observed during the visualization experiments that if the initial state before the abrupt stoppage was turbulent, the turbulence decayed in the matter of couple of seconds (the results are not presented herein). Whereas, Verschoof *et al.* [12] through their experimental PIV and LDA study and Ostilla-Monico *et al.* [9] through their numerical study observed a decay time of 1000 seconds after their gradual stoppage of inner cylinder from a $Re_i = 2 \times 10^6$ compared with the highest tested

Re_i=2.7×10^4 . It should also be noted that their η=0.716 and gap-width d=0.079 m in comparison to the current configuration of η=0.8 and gap-width d=0.01 m. The geometrical configuration and 100 times higher Re_i could be the leading factors for such a discrepancy.

Fig. 2 presents the decay of the azimuthal velocity with time. The azimuthal velocity was averaged axially over 100 mm in the mid-height region, radially over 1.7 mm in the center of gap region and over time for each 1 second. The visualization instantaneous snapshots presented alongside the velocity decay demonstrate the evolution of the generation and decay process. The visualization and PIV velocity estimations were conducted separately and do not necessarily represent the actual time-specific evolution but rather the probability of its observation in that time zone. It is very interesting to not that after the stop, once the decay started it was much faster compared to the gradual decay observed by Verschoof *et al.* [12] and Ostilla-Monico *et al.* [9]. Once again the geometrical configuration of having practically 8 times the current gap-width should be the major reason for having much slower decay in their case or faster in our case due to just 10 mm of gap-width.

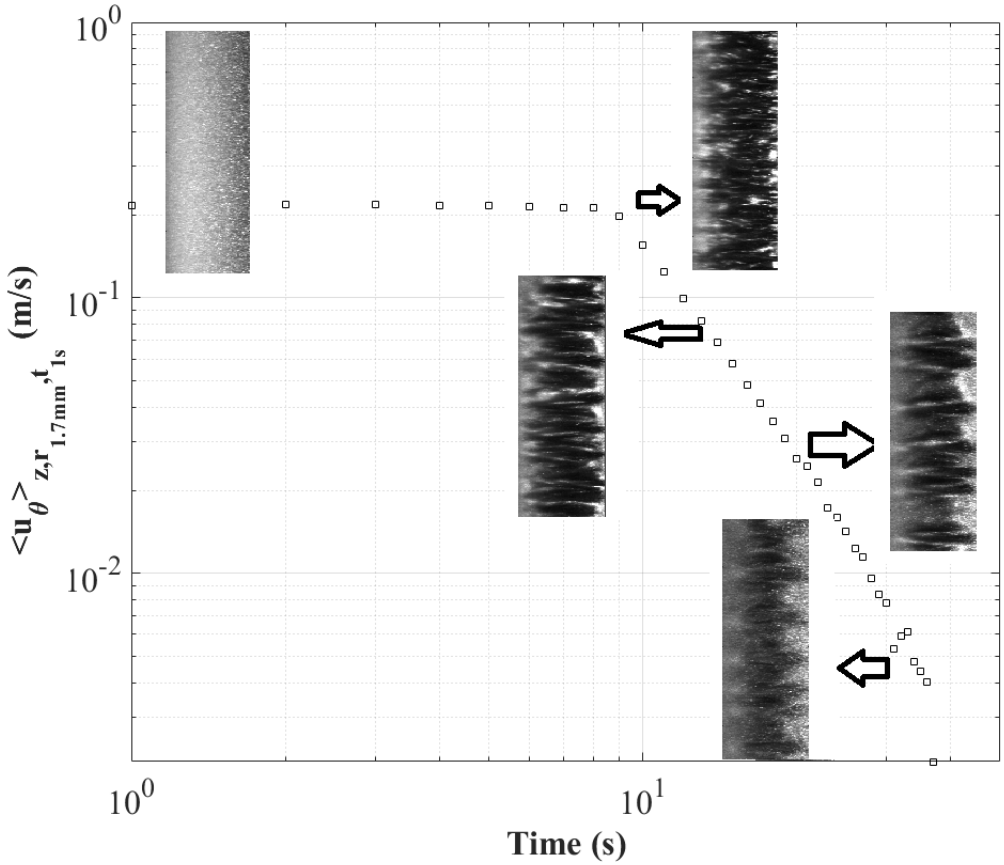

Figure 2. Decay of azimuthal velocity with time. It is averaged axially, radially around the center of gap-width over 1.7 mm and each 1 sec. Snapshots of instantaneous visualizations are also presented to show the evolution of the decay of the velocity.

In the Fig. 3, the decay of azimuthal velocity at different time-steps is shown for different configurations of inner and outer Reynolds number in co- and counter-current situations. The azimuthal velocity is averaged axially and over time for each 1 second, and $R_d = (r - r_i)/d$. A selected few time-steps were

chosen to present the decay of the turbulence. In all cases, the stoppage happened within the first second but not always at the same time ; as a result, the laminar mean profile which was present before the stoppage has been influenced due to the stoppage near the outer cylinder region. Nonetheless, the velocity profile for the 1st second follows very well the analytic laminar profile presented as the dotted line which proves the validity of the stereo-PIV estimations.

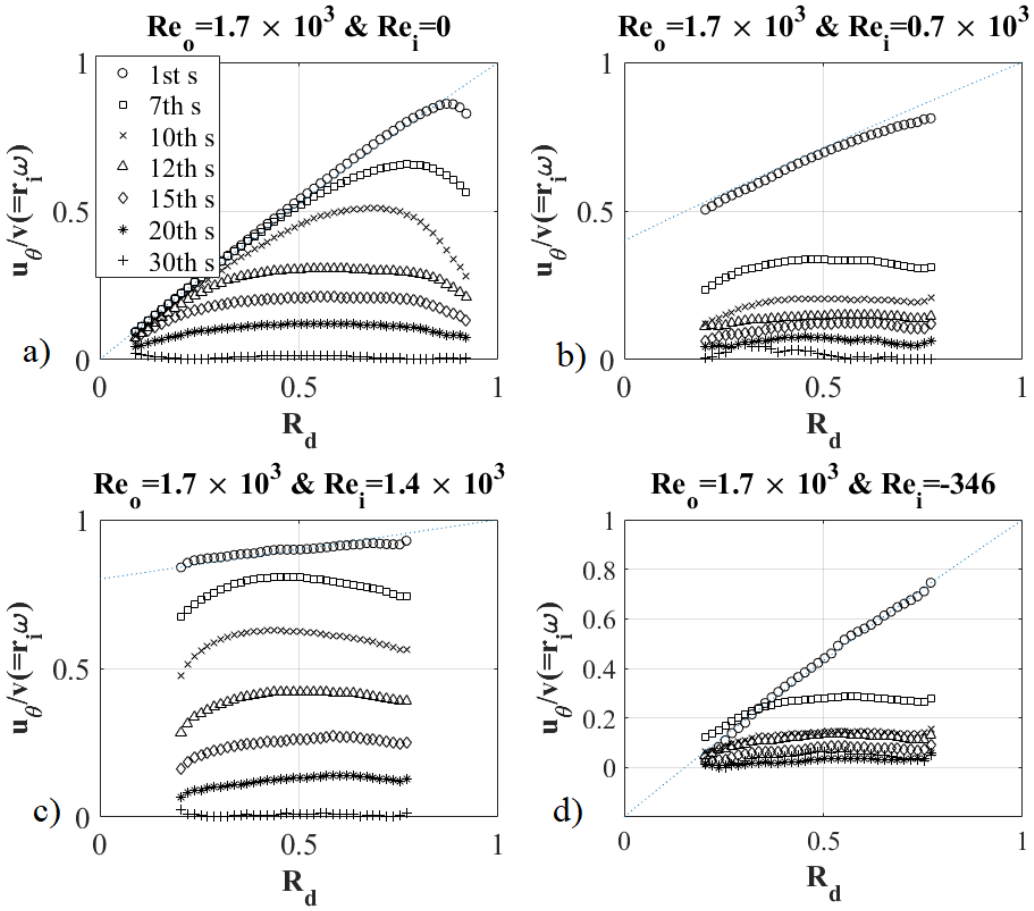

Figure 3. Decay of azimuthal velocity for different co- and counter-current configurations at different time-steps. The legend for the figures in same as that of Fig. a. The dotted line represents the analytic laminar profile.

Another disagreement w.r.t the results of Verschoof *et al.* [12] and Ostilla-Monico *et al.* [9] is that no self-similarity is observed in all the three phases of the decay : first, intermediate and the final phase. Verschoof *et al.* [12] defined the criteria for self-similarity as that when the velocity profiles are normalized, with the mean azimuthal velocity averaged radially and azimuthally, the profiles overlapped each other. They observed self-similarity in the intermediate state, but we didn't observed self-similarity in any of the three stages though the mean azimuthal velocity was averaged axially and radially (the figure is not presented here).

4 Conclusion

In conclusion, a visualization and stereo-PIV analysis is presented for the instantaneous stoppage of cylinders of TC system which leads to the generation and consequently decay of turbulence due to the

absence of any further driving force. The lowest Re_o at which this phenomenon could be observed was found to be 606, which could be further lowered to 433 with the addition of co- or counter rotation. The primary criterion to observe it was the presence of laminar flow prior to the abrupt stoppage. In case the initial flow was turbulent, the turbulence decayed in the matter of couple of seconds. After the abrupt stoppage, the velocity decayed much faster and no self-similarity was observed which has been one of the primary supposition in the case of homogeneous isotropic turbulence and has been observed by George [6]. Nonetheless, many dissimilarities were observed in regard to the results of Verschoof *et al.* [12] and Ostilla-Monico *et al.* [9] which are most probably due to vastly different geometrical configurations for the TC system. These are just first few analyses and have generated a scope for much detailed study, which are currently underway, of this unique phenomenon.

Acknowledgment

We would like to offer our sincere gratitude for financial support from the CPER-FEDER project BIOENGINE.

Références

1. G. I. Taylor, Statistical Theory of Turbulence, *Proc. Roy. Soc. Lon. Ser. A. Math. and Phy. Sci.*, **151**, 421–444 (1935).
2. T. de Karman and L. Howarth, On the Statistical Theory of Isotropic Turbulence, *Phys. Lett. A*, **164**, 192–215 (1938).
3. A. N. Kolmogorov, On degeneration (decay) of isotropic turbulence in incompressible viscous liquid, *Dokl. Akad. Nauk SSSR*, **31**, 538–540 (1941).
4. K. Batchelor Goerge, A. Townsend and G. I. Taylor, Decay of isotropic turbulence in the initial period, *Proc. Roy. Soc. Lon. Ser. A. Math. and Phy. Sci.*, **193**, 539–598 (1948).
5. K. Batchelor Goerge, A. Townsend and G. I. Taylor, Decay of turbulence in the final period, *Proc. Roy. Soc. Lon. Ser. A. Math. and Phy. Sci.*, **194**, 527–543 (1948).
6. W. K. George, The decay of homogeneous isotropic turbulence, *Phys. Fluids A*, **4**, 1492–1509 (1992).
7. H. Touil, J.-P. Bertoglio and L. Shao, The decay of turbulence in a bounded domain, *Les méthodes nouvelles de la mécanique céleste*, **3**, N49 (2002).
8. K. Schneider and M. Farge,Final states of decaying 2D turbulence in bounded domains : Influence of the geometry, *Physica D : Nonlin. Phen.*, **237**, 2228–2233 (2008).
9. R. Ostilla-Mónico, X. Zhu, V. Spandan, R. Verzicco and D. Lohse, Life stages of wall-bounded decay of Taylor-Couette turbulence, *Phys. Rev. Fluids*, **2**, 114601 (2017).
10. T. Schikarski and M. Avila, T mixer a novel system to investigate decaying turbulence in a wall-bounded environment, *16th Eur. Turb. Conf.*, (2017).
11. J. Peixinho and T. Mullin, Decay of Turbulence in Pipe Flow, *Phys. Rev. Lett.*, **2**, 114601 (2017).
12. R. A. Verschoof, S. G. Huisman, R. C. A. van der Veen, C. Sun and D. Lohse, Self-similar decay of high Reynolds number Taylor-Couette turbulence, *Phys. Rev. Fluids*, **1**, 062402 (2016).
13. S. G. Huisman, R. C. A. Van der Veen, C. Sun and D. Lohse, Multiple states in highly turbulent TaylorCouette flow, *Nat. Commun.*, **5**, 3820 (2014).